AN EXPERIMENTAL STUDY ON THE DETERMINATION OF AERODYNAMIC PARAMETERS OF QUARTZ SAND

Phi Manh Ngo*, Thanh Son Tran, Quoc Huy Nguyen

The University of Danang - University of Science and Technology, Vietnam

*Corresponding author: npmanh@dut.udn.vn

(Received: May 18, 2025; Revised: June 11, 2025; Accepted: June 21, 2025)

DOI: 10.31130/ud-jst.2025.23(9B).494

Abstract - Convective drying systems have been increasingly adopted in quartz sand processing, replacing traditional contact drying methods that rely on LPG or coal combustion. In a convective quartz sand dryer, accurate estimation of the pressure drop across the sand bed is critical for selecting appropriate exhaust fans, based on the required airflow rate and pressure head. The Ergun equation is commonly employed to calculate this pressure drop. However, due to the unavailability or variability of key aerodynamic parameters of quartz sand - such as particle size, shape, porosity, and bulk density - the accuracy of predictions using the Ergun equation is often limited. To address this challenge, the present study focuses on developing an experimental apparatus to directly measure the pressure drop across a quartz sand bed under various operating conditions and particle size distributions. The experimental results are compared with values obtained from the Ergun equation to evaluate its applicability.

Key words - Convective dryer; quartz sand; aerodynamic parameters; pressure drop; sand moisture content

1. Introduction

Quartz sand consists mainly of silicon dioxide (SiO_2), typically accounting for more than 95% of its composition. It is formed through natural processes such as weathering, transport, and deposition of quartz-rich rocks, especially quartzite. The particles are usually translucent or milky white and possess high hardness (Mohs scale 7) and excellent resistance to chemical corrosion. Besides SiO_2, small amounts of impurities such as iron, aluminum, and calcium may also be present. High-purity quartz sand - with SiO_2 content exceeding 99.5% - plays an essential role in various industrial applications, including glass production, foundry casting, water treatment, and construction materials [1], [2].

Among the key stages in quartz sand processing, drying is both technically critical and energy-intensive. Conventional drying methods often use direct contact heat transfer with combustion of coal or LPG, which results in high operational costs [3], [4]. To reduce energy consumption, convective drying using air heated indirectly by saturated steam has been increasingly adopted in industrial practice. This method is implemented in drying systems such as rotary drum dryers and fluidized bed dryers [5], [6].

In convective drying systems, air must pass through a packed bed of quartz sand. Accurate determination of aerodynamic parameters - such as bulk density and bed porosity - is essential for predicting the pressure drop across the sand layer, which directly influences the design and selection of exhaust fans used in drying equipment [7]. However, such parameters are often difficult to obtain from the literature or vary significantly depending on the sand's origin and conditions, leading to large discrepancies between theoretical calculations and actual performance.

To address this limitation, the present study introduces a dedicated experimental apparatus designed to directly measure the pressure drop across a quartz sand bed under varying conditions. The obtained results are systematically compared with predictions from the Ergun equation, in which the porosity and bulk density are determined through direct experimentation. This approach enhances the reliability of pressure drop estimations and contributes to the more accurate and energy-efficient design of convective drying systems for quartz sand [8].

2. Experiment

2.1. Materials

The sand samples used in this study were collected from Hoa Hung Loc Materials Production & Trading Co., Ltd., located in Quang Nam Province. A total of eight samples were obtained, as presented in Table 1. After drying, the sand was sieved into six distinct particle size fractions, labeled as Sample 1 through Sample 6, corresponding to the following size ranges: Sample 1 (<0.1 mm), Sample 2 (0.1–0.4 mm), Sample 3 (0.4–0.7 mm), Sample 4 (0.7–1.2 mm), Sample 5 (1.2–2.5 mm), and Sample 6 (>2.5 mm). In addition to these classified samples, two unsieved samples were included for comparison: Sample 7, referred to as "Wet sand", represents the original moist sand before drying and sieving; and Sample 8, referred to as "Dried sand", is the sand after drying (using a tower dryer) but before any size-based classification. These samples were used to investigate the effects of moisture content and particle size on pressure drop characteristics.

Table 1. *Sand samples chosen for experimental investigation*

#	1	2	3	4	5	6	7	8
Size, mm	<0,1	0,1 ÷ 0,4	0,4 ÷ 0,7	0,7 ÷ 1,2	1,2 ÷ 2,5	>2,5	Wet sand	Dried sand

2.2. Experimental Apparatus for Measuring Airflow Pressure Drop Through a Quartz Sand Bed

Figure 1 illustrates the schematic diagram of the experimental apparatus used to measure the airflow resistance through a quartz sand bed. The system comprises key components including a blower, a

differential pressure gauge for measuring the pressure difference ($\Delta P = P_1 - P_2$), air pipes, a support frame, and auxiliary equipment.

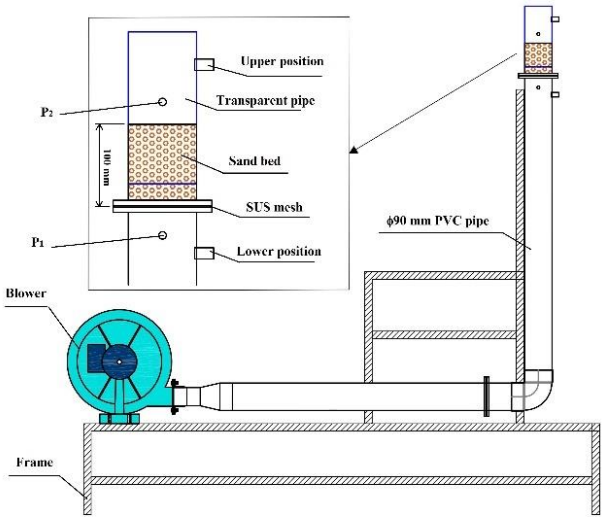

Figure 1. *Experimental setup*

During the experiment, quartz sand is loaded into a vertical transparent mica tube. A stainless-steel mesh is placed at the bottom to prevent sand from falling during testing. Air is blown upward through the sand layer using a fan, and the airflow velocity is controlled by a frequency inverter operating at different frequencies. The differential pressure sensor is connected at two points - above and below the sand bed - to measure the pressure drop across the sand layer, which corresponds to its flow resistance.

A magnesense pressure sensor is used to measure the pressure of air and compatible gases. It offers high accuracy of up to ±1% FSO (Full Scale Output), with an operating temperature range from -4 to 158°F (-20 to 70°C), a pressure measurement capacity of up to 6 psi (41368.5 Pa), and a response time of approximately 3 seconds.

The pressure drop across the quartz sand bed (ΔP) was experimentally measured for eight different samples, as listed in Table 1, under various inlet air velocities. The airflow velocity was controlled by adjusting the frequency of the blower fan. The air velocities before and after the sand layer were directly measured at the lower and upper positions of the bed, respectively, as illustrated in Figure 1, using the Testo 425 anemometer. This device offers a measurement range from 0.01 to 30 m/s, with an accuracy of ±(0.03 m/s + 4.0% of the measured value) for velocities from 0.01 to 20 m/s.

2.3. Determination of porosity (ε) and bulk density of sand bed

The porosity and bulk density of the quartz sand bed were experimentally determined using eight sand samples, as presented in Table 1. The procedure for measuring the porosity is illustrated in Figure 2. Each measurement was repeated three times, and the reported results represent the average of these three trials. For this experiment, a 50 mL graduated measuring cup and a Vibra AJ analytical balance with a precision of up to 0.001 g were employed.

Steps for measuring and calculating the porosity of a sand bed:

Step 1: Weigh the empty beaker to determine its mass m_b, in grams (g).

Step 2**:** Fill the beaker with sand until the sand reaches a height of 30 mL. Weigh the beaker and sand (m_s) together to determine the combined mass m_b+m_s, in grams (g).

Step 3**:** Add water to the cup without changing the total height (still 30 mL). The water will fill the voids between sand particles. Weigh the beaker again (now containing sand and water) to determine the total mass ($m_b+m_s+m_w$), from which the mass of the water (m_w) can be deduced.

Step 4: Calculate the volume of water V_w occupying the void space in the sand layer using the formula:

$$m_w = V_w.\rho_w \Rightarrow V_w = m_w / \rho_w \quad (1)$$

Thus, the porosity (ε, %) of the sand bed is calculated as:

$$\varepsilon = \frac{V_w}{V_s} \times 100 \quad (2)$$

Where:

V_s is the total bulk volume of the sand layer (in this case, 30 mL),

ρ_w is the density of water (1 g/mL at room temperature).

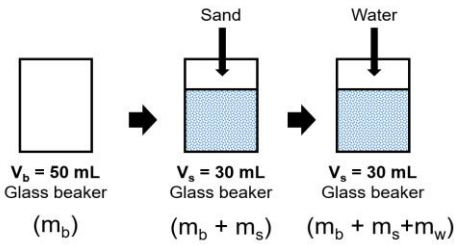

Figure 2. *Procedure for determining the porosity of the sand bed*

Simultaneously, the bulk density of the quartz sand bed (ρ_s, kg/m^3) was calculated using Equation (3) below:

$$\rho_s = \frac{m_w}{V_s} \quad (3)$$

3. Result analysis

3.1. Porosity and bulk density of the bed sand

The porosity of the quartz sand bed is significantly influenced by particle size. As illustrated in Figure 3, the porosity varies between 35.70% and 41.72% across different particle size fractions. Specifically, the porosity increases from 36.95% for particles smaller than 0.1 mm to 41.72% for particles larger than 2.5 mm. A noticeable drop is observed at the 0.7–1.2 mm range, where porosity reaches a minimum of 35.70%. This trend is in line with previous findings by Islam and Skalle (2013), who reported that well-sorted quartz sands exhibit porosity values in the range of 35–45%, and that porosity tends to increase with larger particle size due to less efficient packing [9].

This behavior can be explained by the geometric arrangement of the particles: finer sands tend to pack more densely due to better interlocking and fewer voids, while coarser particles create more intergranular space, thus increasing porosity. The fluctuation in the 0.7–1.2 mm range

may reflect a transitional zone where packing efficiency is locally maximized due to optimal grain interlocking.

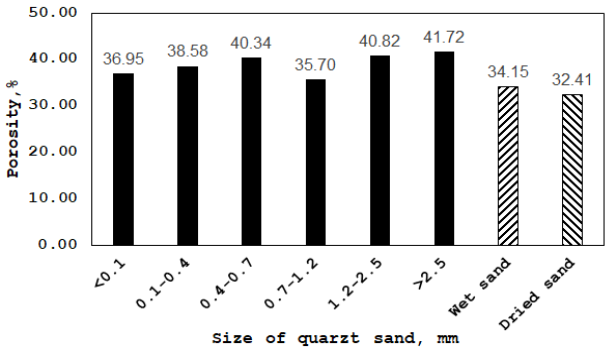

Figure 3. *Porosity of the bed sand at different particle size fractions*

When this trend in porosity is analyzed alongside the bulk density data (Figure 4), an inverse correlation becomes evident. The bulk density of the sand bed generally decreases as porosity increases. For instance, the bulk density reaches a maximum of 1,400 kg/m³ for particles smaller than 0.1 mm, where the porosity is relatively low (36.95%), and decreases to 1,251 kg/m³ for particles larger than 2.5 mm, corresponding to the highest porosity value (41.72%). This inverse relationship is consistent with the results of Nardelli et al. (2016), who demonstrated through experimental and DEM simulation methods that an increase in porosity corresponds to a decrease in bulk density for quartz sands [10].

The consistency between the measured porosity and bulk density in this study and values reported in the literature confirms the reliability of the experimental procedures. The measured range of bulk density (1,251–1,400 kg/m³ for dry sands) also falls within the expected range reported by Ahrens and Yang et al. for similarly graded quartz sands, with typical bulk densities between 1,300 and 1,500 kg/m³ [11, 12].

These findings validate the experimental approach employed in this study and confirm the strong influence of particle size on the physical structure of the granular bed. Moreover, the slightly lower porosity observed in wet and dried samples (34.15% and 32.41%, respectively) compared to loose dry packing may reflect densification due to handling or moisture-mediated rearrangement during sample preparation.

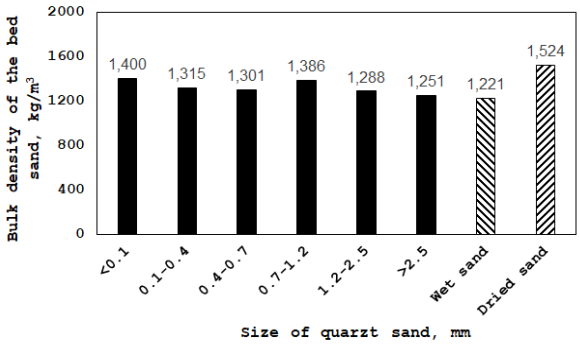

Figure 4. *Bulk density of the bed sand at different particle size fractions*

3.2. Pressure drop of air through the bed sand

Our experimental data (Table 2) demonstrate that the pressure drop across the sand bed (ΔP) is inversely related to the particle size. It is important to note that experiments could not be performed on sand with particle sizes below 0.1 mm. This limitation arose due to the extremely high flow resistance of such fine particles, which rendered the airflow through the bed negligible even at low fan frequencies. The high interparticle cohesion and reduced pore size.

Additionally, airflow tests were restricted to fan frequencies up to 40 Hz. At higher frequencies, particularly near 50 Hz, the gas velocity was observed to induce partial fluidization or "incipient boiling" behavior in the bed, especially for coarser sand fractions. This onset of fluidization disrupted steady pressure drop measurements and marked the upper boundary of the fixed-bed regime under our laboratory conditions.

At a given superficial air velocity (v), sand with smaller particles (e.g., 0.1–0.4 mm) exhibits significantly higher pressure drops than beds composed of larger particles (e.g., 1.2–2.5 mm or >2.5 mm). For instance, at an excitation frequency of 35 Hz (v ≈ 0.15–0.17 m/s), the pressure drop for the 0.1–0.4 mm sand reaches 503.8 Pa, while that of the >2.5 mm fraction is only 449.3 Pa, despite a similar superficial velocity.

This trend aligns with the observed porosity values (Figure 3), which increase with particle size. Finer sand fractions (e.g., <0.1 mm and 0.1–0.4 mm) have lower porosity (36.95% and 38.58%, respectively), resulting in narrower interstitial flow channels and greater surface area contact between particles and gas, hence higher flow resistance. In contrast, coarser sand (>2.5 mm) has a porosity of 41.72%, allowing for more efficient gas percolation through the bed.

These findings are in agreement with previous studies. Yang et al. [13] reported that permeability increases and pressure drop decreases with both increasing grain size and broader grain-size distribution. Nardelli et al. [10] confirmed that quartz beds composed of larger, more spherical particles exhibit reduced tortuosity and higher void ratios, which facilitate gas flow and reduce aerodynamic resistance. The consistency between our results and literature enhances the reliability of our experimental methods.

Additionally, a comparison of pressure drop between wet sand and dried sand at frequencies of 30 Hz, 35 Hz, and 40 Hz reveals noticeable differences. At 30 Hz, the pressure drop for wet sand is 368.7 Pa, whereas dried sand exhibits a slightly higher value of 380.9 Pa. At 35 Hz, wet sand shows 503.5 Pa, while dried sand reaches 511.9 Pa. Similarly, at 40 Hz, the pressure drop for wet sand is 652.3 Pa, compared to 653.1 Pa for dried sand. These results indicate that dried sand generally shows a slightly greater pressure drop than wet sand under the same airflow conditions. This can be explained by the physical behavior of wet sand particles: when wet, the particles tend to adhere to one another due to surface tension, forming small agglomerates with larger voids between them. In contrast,

dried sand particles are more likely to remain separate and densely packed, creating more resistance to airflow through the bed.

However, the difference in pressure drop between wet and dried sand is not substantial, which can be attributed to the relatively small difference in moisture content. Specifically, the dried sand has a moisture content of approximately 0.3%, while the wet sand contains about 6–7% moisture.

Table 2. *Pressure drop through the sand bed at different particle size fractions*

Size, mm	Frequency, Hz					
	20		25		30	
	v, m/s	ΔP, Pa	v, m/s	ΔP, Pa	v, m/s	ΔP, Pa
0.1 - 0.4	0.03	168.5	0.03	263.7	0.04	384.3
0.4 - 0.7	0.05	161.4	0.07	260.1	0.09	371.8
0.7 - 1.2	0.10	158.9	0.14	253.6	0.17	369.8
1.2 - 2.5	0.16	157.3	0.25	253.5	0.30	367.9
>2.5	0.63	155.0	0.83	249.0	1.07	365.0
Wet sand	0.26	161.2	0.40	260.6	0.56	368.7
Dried sand	0.10	163.9	0.09	254.1	0.15	380.9
Size, mm			35		40	
			v, m/s	ΔP, Pa	v, m/s	ΔP, Pa
0.1 - 0.4			0.05	503.8	0.05	695.9
0.4 - 0.7			0.11	502.5	0.10	692.0
0.7 - 1.2			0.22	501.7	0.20	670.1
1.2 - 2.5			0.55	499.9	0.60	662.8
>2.5			1.19	495.1	1.27	659.9
Wet sand			0.63	503.5	0.68	652.3
Dried sand			0.15	511.9	0.17	653.1

Overall, these results highlight that both particle size and porosity critically influence the flow resistance through granular media. Our observations conform to classical models such as the Ergun equation and Kozeny–Carman model, which predict higher pressure drops for smaller particles and lower porosity media.

Subsequently, we compared the measured pressure drop across the sand bed with the values predicted by the Ergun equation (4). This comparison was carried out for two sand size ranges - 1.2–2.5 mm and greater than 2.5 mm (as shown in Table 1) - at three superficial air velocities corresponding to fan motor frequencies of 30, 35, and 40 Hz.

The Ergun equation is widely used to estimate the pressure drop across a packed bed of particles for both laminar and turbulent flow regimes [14]:

$$\Delta P = L.\left(\frac{150.\mu.(1-\varepsilon)^2.v}{\varepsilon^3.{d_p}^2} + \frac{1{,}75.\rho.(1-\varepsilon).v^2}{\varepsilon^3.d_p}\right) \quad (4)$$

Where:

ΔP: Pressure drop across the sand bed (Pa).

L: Thickness of the sand bed (m); in this study L = 0.1 m.

d_p: Mean sand diameter (m) which was determined as the average value within each sand size range. For instance, for the size fraction 0.1–0.4 mm, the mean diameter was calculated as (0.1+0.4)/2=0.25 mm. This approach was applied consistently across all particle size fractions.

μ: Dynamic viscosity of the air (Pa·s).

ρ: Density of the air (kg/m³).

v: Superficial velocity of the air before entering the bed (m/s).

ε: Porosity (void fraction) of the bed (dimensionless).

The physical properties of air in Equation (4), such as dynamic viscosity and density, were determined based on room temperature conditions at 25 °C. The particle diameter was taken as the average value within each size range, and the bed porosity was obtained from the experimental measurements presented in Figure 3.

Figures 5a and 5b illustrate the pressure drop of airflow through packed beds of sand with two different particle size ranges, 1.2–2.5 mm and >2.5 mm, respectively. In each figure, the pressure drop was measured experimentally and also predicted using the Ergun equation at different superficial air velocities.

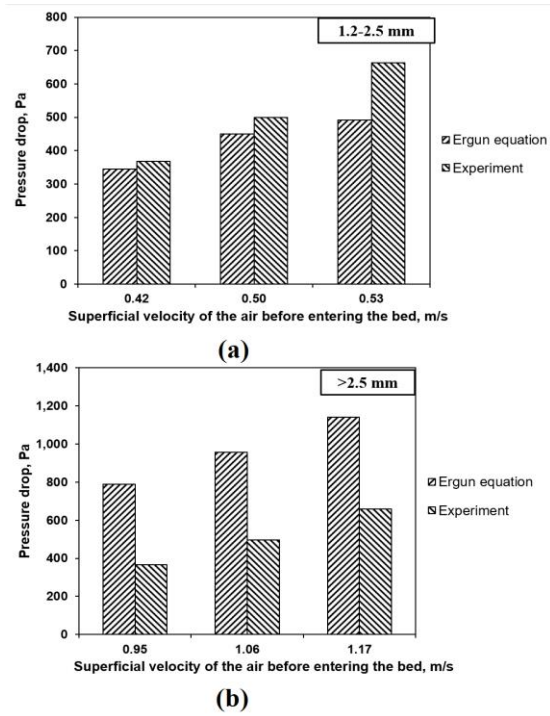

Figure 5. *Comparison pressure drop between experiment and Ergun's equation*

For the particle size range of 1.2–2.5 mm (Figure 5a), the pressure drop predicted by the Ergun equation (345.4–491.8 Pa) was in relatively close agreement with the experimental data (367.9–662.8 Pa). The difference between predicted and measured values increased with increasing air velocity. For instance, at an air velocity of 0.42 m/s, the model predicted 345.4 Pa while the experimental result was 367.9 Pa - a difference of only 6.1%. However, at 0.53 m/s, the predicted value was 491.8 Pa, whereas the experimental result reached 662.8 Pa, corresponding to a 25.8% underprediction.

In contrast, for the larger particle size range (>2.5 mm, Figure 5b), the Ergun equation significantly overestimated the pressure drop across all tested velocities. At 0.95 m/s, the predicted pressure drop was 788.8 Pa compared to only 365.0 Pa measured experimentally - an overprediction of more than 116%. At the highest air velocity of 1.17 m/s, the predicted value reached 1,140 Pa, while the measured pressure drop was 659.9 Pa, representing a 72.8% difference.

These results demonstrate that the Ergun equation becomes less reliable when applied to larger particle sizes in this study. This discrepancy is attributed to the fact that the Ergun equation assumes idealized conditions, including uniform spherical particles and homogeneous packing. In this study, a sphericity factor of 1 was assumed, though real sand grains are typically irregular in shape. Moreover, accurate inputs for bed porosity and particle diameter are essential for reliable predictions using the Ergun model.

The significant overprediction observed for coarse particles suggests that the flow behavior in such beds deviates considerably from the assumptions inherent in the Ergun formulation. Therefore, the use of the Ergun equation in this context should be approached with caution, and experimental validation is highly recommended.

Importantly, the experimental apparatus developed in this study allows for the direct and accurate measurement of airflow resistance through granular beds, regardless of variations in particle size, shape, or bed porosity. This experimental approach offers a practical advantage over purely theoretical models when evaluating pressure losses in real-world applications involving non-ideal granular media.

4. Conclusion

In this study, a practical method was developed to determine the porosity and mass of quartz sand beds based on eight samples collected from an actual industrial plant. The measured values showed good agreement with previously published data, confirming the reliability and consistency of the experimental procedure.

In addition, a custom-designed apparatus was successfully constructed to measure the pressure drop of airflow through static beds of quartz sand. This device enables accurate determination of pressure loss under realistic conditions, accounting for actual particle size fractions and packing configurations found in industrial applications.

A comparison between experimental results and theoretical predictions using the Ergun equation highlighted both the strengths and limitations of the model. While the Ergun equation provided reasonable estimates for finer sand particles (1.2–2.5 mm), it significantly overpredicted the pressure drop for coarser particles (>2.5 mm), suggesting that its underlying assumptions may not hold for irregular or non-spherical granular media.

These findings underscore the importance of experimental validation, particularly when dealing with non-ideal materials such as natural quartz sand. The developed experimental system offers a robust and effective tool for accurately assessing flow resistance in granular media, beyond the constraints of classical empirical models like Ergun's equation.

Acknowledgments: This research is funded by The University of Danang – University of Science and Technology under project code T2023-02-27.

REFERENCES

[1] Bokela GmbH, "Glass Sands", *Bokela.com*, 2023. [Online]. Available: https://www.bokela.com/en/quartz-sand [Accessed Sept. 02, 2025].

[2] Sunco Machinery, "Silica Sand Dryer", *SuncoDrying.com*, 2020. [Online]. Available: https://www.suncodrying.com/other-drying-machine/20200324/8.html [Accessed Sept. 02, 2025].

[3] Tema Process, "Sand Drying", *TemaProcess.com*, 2022. [Online]. Available: https://temaprocess.com/2022/sand-drying/ [Accessed Sept. 02, 2025].

[4] LZZG, "Frac Sand Cleaning and Drying Process", *LZZGMachine.com*, 2023. [Online]. Available: https://www.lzzgmachine.com/service-parts/product-knowledge/frac-sand-cleaning-and-drying-process.html [Accessed Sept. 02, 2025].

[5] A. Momeni and K. Sadeghi, "Experimental study of convective drying characteristics of a wet porous sand layer", *International Journal of Heat and Mass Transfer*, vol. 137, pp. 1052–1062, 2019.

[6] M. Khazaei and H. Majdi, "Porosity-Dependent Drying Behavior of Quartz Sand Using Whitaker Model in Convective Drying", *Processes*, vol. 12, no. 2, p. 337, 2024.

[7] D. Y. Chena and J. Y. Xue, "Influence of drying methods on the thermodynamic parameters: Effective moisture diffusion and drying rate of silica sand", *Academia.edu*, 2023. [Online]. Available: https://www.academia.edu/113342703 [Accessed Sept. 02, 2025].

[8] McLanahan Corporation, "Frac Sand Drying Methods: Rotary vs. Fluid Bed", *PowderBulkSolids.com*, 2021. [Online]. Available: https://www.powderbulksolids.com/drying/frac-sand-drying-methods-rotary-vs-fluid-bed [Accessed Sept. 02, 2025].

[9] M. Islam and P. Skalle, "Laboratory measurement of total porosity in unconsolidated quartz sand by two integrated methods", *Journal of Petroleum & Environmental Biotechnology*, 2013. [Online]. Available: https://www.longdom.org/open-access-pdfs/laboratory-measurement-of-total-porosity-in-unconsolidated-quartz-sand-by-two-integrated-methods-2381-8719-1000448.pdf [Accessed Sept. 02, 2025].

[10] V. Nardelli, S. Imposimato, F. Montagnaro, and P. Salatino, "Micro–macro properties of quartz sand: experimental investigation and DEM simulations", *Powder Technology*, vol. 289, pp. 57–68, 2016. https://doi.org/10.1016/j.powtec.2015.11.036

[11] T. J. Ahrens, *Mineral Physics and Crystallography: A Handbook of Physical Constants*, AGU Reference Shelf 2. Washington, DC: American Geophysical Union, 1995.

[12] S. Yang, Y. Li, Q. Liu, and H. Wang, "An experimental insight into the influence of sand grain size distribution on rock porosity and permeability", *Journal of Petroleum Science and Engineering*, vol. 213, 2022. https://doi.org/10.1016/j.petrol.2022.110514

[13] S. Ergun, "Fluid flow through packed columns", *Chemical Engineering Progress*, vol. 48, no. 2, pp. 89–94, 1952..